Available online on www.ijcpr.com
International Journal of Current Pharmaceutical Review and Research; 7(6); 347-359

ISSN: 0976 822X

Research Article

Assessment of Mutagenicity Induced by Toxic Factors Affecting Ovarian Tissue in Rats by Electrophoresis and Molecular Dynamic Modeling

Wael M Aboulthana[1*], Mohamed Ismael[2], Hatem S Farghaly[3]

[1]*Biochemistry Department, Genetic Engineering and Biotechnology Division, National Research Centre, 33 Bohouth Street, Dokki, Giza, Egypt affiliation ID: 60014618.*
[2]*Energy and Environmental Sciences Laboratory, Chemistry, Department, Faculty of Science, Sohag University, Egypt.*
[3]*Department of Biochemistry, Faculty of Pharmacy, Nahda University, Beni-Sueif, Egypt.*

Available Online: 25th December, 2016

ABSTRACT
Lithium carbonate (Li_2CO_3) and lead acetate (Pb_2COOH) belong to the female reproductive toxicants that cause infertility through the interference with development of growing follicles in the ovarian tissue. Doxorubicin (Dox) and cyclophosphamide (CPA) are considered as the most effective chemotherapeutic drugs which are associated with the greatest risk of female infertility. Furthermore, whole body gamma irradiation for therapeutic purpose by mean of radiotherapy affected female reproductive organ through destruction of the small and antral follicles. The present study aimed to reveal the deleterious effect of all of these (toxic) substances factors on the cellular macromolecules which separated and identified electrophoretically in the ovarian tissue. During the present study, the toxic factors exhibited qualitative abnormalities represented by disappearance of normal bands and appearance of one or more of abnormal bands. Otherwise, the alterations may occur at the quantitative level through remaining the normal bands but with changing the band quantity. The similarity index (SI) is only correlated to the qualitative alterations. In the electrophoretic protein pattern, the lowest SI value (0.52) was recorded with CPA-treated group and the highest SI value (0.91) noticed with Pb-treated group. In the electrophoretic lipoprotein pattern, there were severe alterations. It was observed that all the bands in the Dox-treated and CPA-treated groups were not matched with all bands of the other groups. In catalase (CAT) pattern, The Pb-treated group is completely identical to control group in number and arrangement of the bands (SI value 1.0). The lowest SI value (0.57) was observed with CPA-treated and Irradiated groups. In peroxidase (POX) pattern, the lowest SI value (0.22) was observed with CPA-treated group and the highest value (0.86) was recorded with Irradiated group. In esterase (EST) pattern, the lowest SI value (0.29) was recorded with the Pb-treated group and the highest SI vale (0.80) was noticed with the Li_2CO_3-treated group. In addition, there was complete similarity between the Dox-treated and Irradiated groups and between CCl_4-treated and CPA-treated groups. It was postulated that the 3D model of the prolactin receptor specific protein (PRAP) which was built using homology modeling showed that PRAP has large amount of loops. It is expected to be very flexible protein and less stable.

Keywords: Lithium Toxicity, Carbon Tetrachloride Toxicity, Lead Toxicity, Doxorubicin, Cyclophosphamide, Irradiation, Prolactin Receptor Specific Protein, Isoenzymes.

INTRODUCTION

Environmental factors exert deleterious effects by enhancing the oxidative stress directly or indirectly through generation of reactive oxygen species (ROS) in both unstressed and stressed cells[1,2]. Rates of production and destruction of ROS were well balanced under normal conditions. However, under stress conditions, the oxidative stress stimulated due to the misbalance through which rate of ROS generation is more rapid than scavenging and detoxifying[3]. It was demonstrated that the exposure to environmental stressors caused alterations in the relative compositions of the antioxidant enzymes[4,5]. Catalase (CAT) and peroxidase (POX) are the most efficient antioxidant enzymes due to their critical role against oxidative stress induced by environmental factors[6]. The normal cells have a variety of defense mechanisms that ameliorate efficiency of the antioxidant enzymes to prevent intracellular damage occurred as a result of ROS attack[7]. The free radicals cause severe alterations in the intracellular macromolecules such as proteins, lipids and DNA. Proteins are responsible for all biological functions occurred inside the cells. The alterations in the native protein pattern are considered as an important part of physiological response to toxic environmental factors[8]. Modified proteins may be removed by normal cellular turnover, but DNA damage requires specific repair mechanisms. When the genomic DNA is the target of oxidation reaction, it can lead to various mutagenic effects

**Author for Correspondence: wmkamel83@hotmail.com*

represented by rearrangements and transcriptional errors that stimulate altering expression of different genes[9]. Lithium carbonate (Li_2CO_3) has been used in medicine as an effective drug for curing bipolar disorders, psychiatric and neurological diseases[10,11] as well as an adjuvant substance in therapy of thyroid disorders[12]. It was documented that lithium affected ovary of the adult rats through decline ovarian steroidogenic enzymes and hence lowering the folliculogenesis process. Two weeks of lithium treatment was sufficient to induce toxicity of the female reproductive organs[13,14]. It was reported that lead acetate (Pb_2COOH) belongs to the reproductive toxicants which cause female infertility through the interference with development of growing follicles in the ovary[15]. Although alkylating chemotherapeutic drugs and irradiation are used in treating various cancerous diseases through induction of DNA damage in cancer cells, these treatments have undesired detrimental side effects on the reproductive system[16]. Doxorubicin (Dox) and cyclophosphamide (CPA) belong to numerous chemotherapeutic drugs[17]. Meirow *et al.*[18] suggested that the mature follicles are the most sensitive target to these chemotherapeutic drugs. Dox is an anthracycline antibiotic used as a potent antineoplastic agent to treat hematological and solid tumours[19,20]. It was postulated that Dox affected the ovaries which served as a tool for tracking down the whole organ pattern of the Dox gonadotoxic effect. For this reason, Ben-Aharon *et al.*[21] recommended that further studies needed in the future to shield the ovaries from chemotherapy peril. It was documented that CPA is one of the most effective alkylating agents which are associated with the greatest risk of female infertility[22]. It targeted primordial and primary follicles. It caused destruction of primordial follicles after one week of treatment by enhancing apoptosis in ovarian follicles. Although the active metabolites of CPA are detoxified by conjugation with glutathione (GSH), the GSH depletion does not seem to be the mechanism by which CPA causes follicular apoptosis[23]. In addition, according to *in vivo* studies which performed in rats and mice, it was found that the whole body gamma radiation exposure by mean of radiotherapy destroys small follicles as well as antral follicles[24]. Prolactin (PRL) is composed of polypeptide hormone and produced primarily in the anterior lobe of pituitary gland[25]. It plays a vital role in promoting follicular development and its effects are mediated by the prolactin receptor (PRLR)[26,27]. Expression of the gene which is responsible for synthesis of PRLR increases during the ovarian development. The PRLR affects the follicular development and maturation[28]. The PRLR protein is expressed in oocytes and prenatal follicles to increase rate of the oocyte maturation and regulate the reproduction process[29,30]. According to the crystal structure of PRLR, the computer modeling and simulation showed that there are minor changes in the tertiary structure of the extracellular subdomain 1 upon disruption of disulfide bond which propagated to the quaternary structure of the homodimer. These changes explain a structural basis for lack of inhibitory function of PRLR[31]. The present study aimed to investigate the deleterious effect of various toxic factors on the native electrophoretic protein, lipoprotein and isozymes in the ovarian tissue of rats. This was in association with the 3D models of the PRLR which was built using homology modeling to give a first insight about the structural characteristics of the activated regions in it.

MATERIALS AND METHODS

Materials: Chemicals and Reagents

Acrylamide, Bis-acrylamide, Ammonium persulfate (APS), N,N,N,N-Tetramethylethylnediamine (TEMED), Coomassie Brilliant Blue G-250 (CBBR-250) and Sudan Black B (SBB) were purchased from Sigma-Aldrich. Cyclophosphamide (CPA), Doxorubicin (Dox), Lead Acetate Trihydrate, Carbon Tetrachloride (CCl_4), Lithium Carbonate (Li_2CO_3) and Benzidine were procured from Sigma Chemicals Company (London, UK). The chemicals used for in-gel esterase staining including α- and β-naphthylacetate, Fast Blue RR were purchased from Qualigens Fine Chemicals, India. All other chemicals and reagents used were of analytical grade and of highest purity.

Animals and Treatments

Seventy adult female rats (weighing between 150-170 gm per one) were housed in the animal house laboratory of national research centre. Each group contains 10 rats. All the animals kept under normal environmental and nutritional conditions at 25 ± 2°C. All the experimental procedures were carried out according to the ethical protocol which followed the ethical guidelines and approved by the institutional animal care of National Research Centre, Dokki, Giza, Egypt.

Experimental Design

The rats were randomly divided into 7 groups. Group I (Control group): Rats were fed with normal diet as *ad libitum* and received distilled water for 60 days. Group II (Pb-treated group): Rats received lead acetate at concentration of 30 mg/kg body weight orally by gavage tube for 60 days by gavage tube[32]. Group III (Li_2CO_3-treated group): Rats were treated with lithium carbonate solution interperitoneally (i.p.) at three dosages of 60,120

PTSX--------PQTQG----LAKD-------AWEIPRESL

PT + PQ+ GL + AE + S

PTRRTFLDPQSCGDLLQAVHLFAKELDAKSV

Figure 1: An alignment between two sequences. Conserved amino acids are aligned and insertions are marked with dashes.

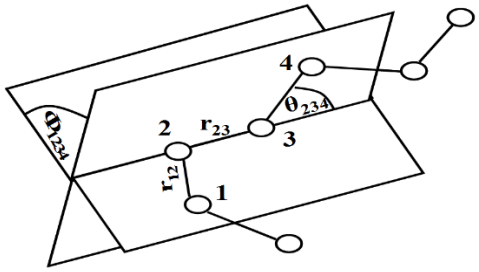

Figure 2: Geometry of a simple chain molecule, illustrating the definition of interatomic distance r_{23}, bend angle θ_{234}, and torsion angle Φ_{1234}.

And
180

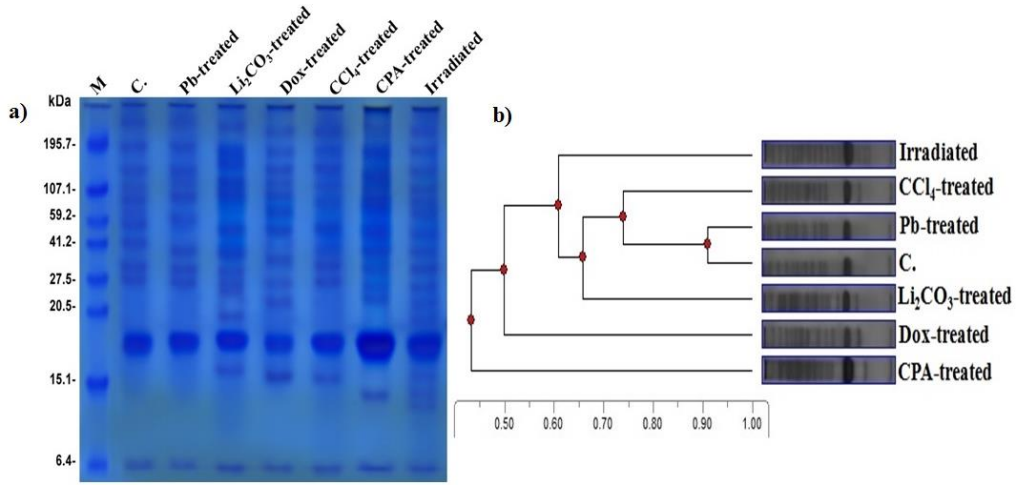

Figure 3: (a) Electrophoretic protein pattern showing toxic effect of Pb_2COOH, Li_2CO_3, Dox, CCl_4, CPA and irradiation on protein pattern in ovarian tissue of female rats, (b) Dendogram showing the similarity and relatiohship among Pb-treated, Li_2CO_3-treated, Dox-treated, CCl_4-treated, CPA-treated and Irradiated groups in female rats as compared to control.

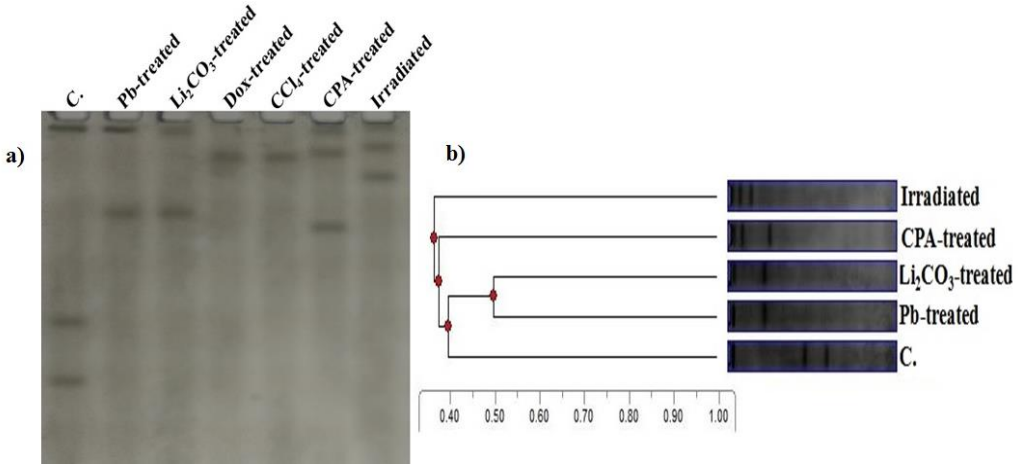

Figure 4: (a) Electrophoretic lipoprotein pattern showing toxic effect of Pb_2COOH, Li_2CO_3, Dox, CCl_4, CPA and irradiation on protein pattern in ovarian tissue of female rats, (b) Dendogram showing the similarity and relatiohship among Pb-treated, Li_2CO_3-treated, Dox-treated, CCl_4-treated, CPA-treated and Irradiated groups in female rats as compared to control.

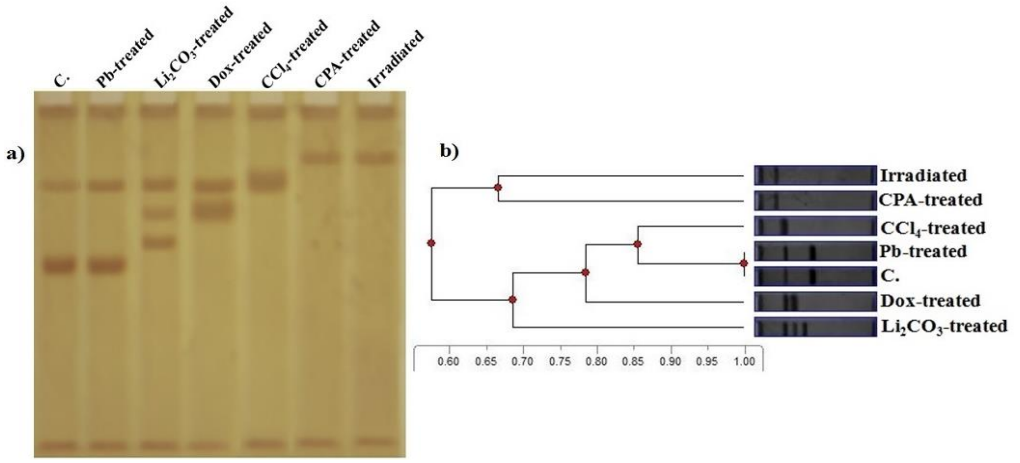

Figure 5: (a) Electrophoretic CAT pattern showing toxic effect of Pb_2COOH, Li_2CO_3, Dox, CCl_4, CPA and irradiation on protein pattern in ovarian tissue of female rats, (b) Dendogram showing the similarity and relatiohship among Pb-treated, Li_2CO_3-treated, Dox-treated, CCl_4-treated, CPA-treated and Irradiated groups in female rats as compared to control.

mg/kg B.W for 21 days[33]. Group IV (Dox-treated group): Rats received Dox at dose level of 25mg/kg b.wt for three times per week for two weeks[34]. Group V (CCl_4-treated group): Rats were injected with CCl_4 i.p. at the dose 0.5 ml/kg b.w. (50 % CCl_4 in olive oil) twice a week for 28 days[35]. Group

VI (CPA-treated group): Rats received CPA i.p. at 40 mg/kg b.w. twice a week for 15 days[36]. Group VII (Irradiated group): Rats were exposed to single dose of 7 Gy delivered at the dose rate of 1.167 Rad / Sec. at Middle Eastern Regional Radioisotope Centre for the Arab Countries, Dokki, Egypt using Cobalt 60 (Co^{60})[37].

Extraction of ovarian tissue homogenates

All the animals were anaesthetized and killed by decapitation. Ovaries were quickly dissected and cleaned carefully from superficial fatty layer and then washed in ice-cold saline. As reported by **Elshawi *et al.*[38]**, the ovaries were freezed rapidly with liquid nitrogen then homogenized in 1 ml water-soluble extraction buffer. The homogenates vortexed for 15 seconds then centrifuged at 10,000 rpm at 4˚C for 15 min. The clear supernatants containing water-soluble proteins were transferred to new eppendorf tubes and kept at deep-freeze until the electrophoretic patterns.

Determination of protein concentration

All samples of each group were pooled together and used as one sample. Protein concentration was estimated in the ovarian tissue homogenates according to method described by Bradford[39] using bovine serum albumin as standard. The protein concentration in each well should be in the range between 60-80 µg protein. Equal quantities of protein were loaded in all wells.

Electrophoretic protein and lipoprotein patterns

To determine the relative mobility (Rm), molecular weight (Mwt) and band percent (Ba %) of the isolated proteins and lipoproteins, the native 10 % polyacrylamide gel electrophoresis of samples was carried out according to method suggested by Laemmli[40] using Mini-gel

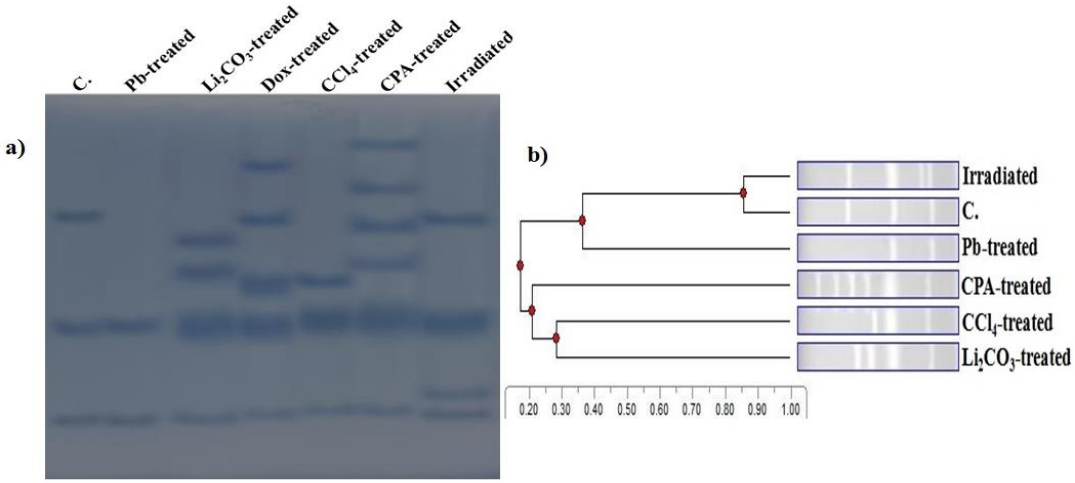

Figure 6: (a) Electrophoretic POX pattern showing toxic effect of Pb_2COOH, Li_2CO_3, Dox, CCl_4, CPA and irradiation on protein pattern in ovarian tissue of female rats, (b) Dendogram showing the similarity and relatiohship among Pb-treated, Li_2CO_3-treated, Dox-treated, CCl_4-treated, CPA-treated and Irradiated groups in female rats as compared to control.

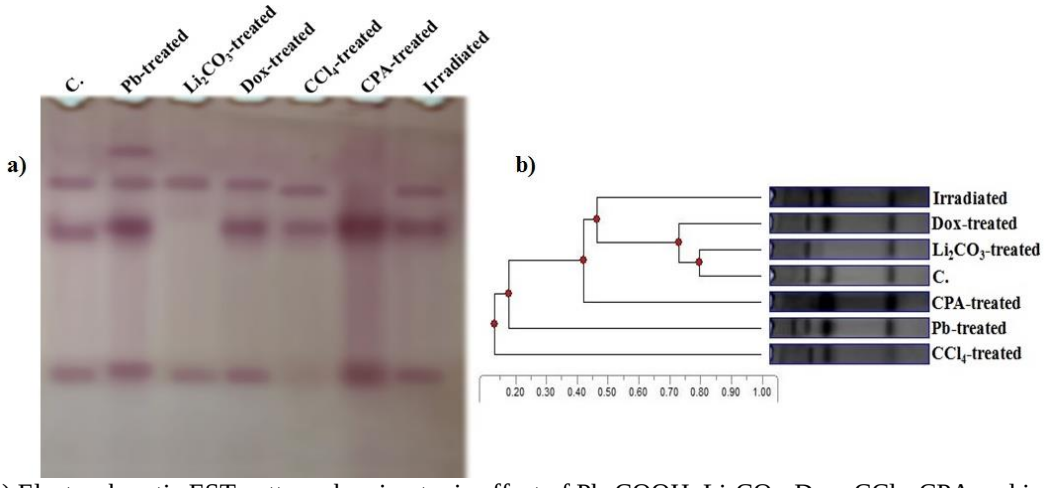

Figure 7: (a) Electrophoretic EST pattern showing toxic effect of Pb_2COOH, Li_2CO_3, Dox, CCl_4, CPA and irradiation on protein pattern in ovarian tissue of female rats, (b) Dendogram showing the similarity and relatiohship among Pb-treated, Li_2CO_3-treated, Dox-treated, CCl_4-treated, CPA-treated and Irradiated groups in female rats as compared to control.

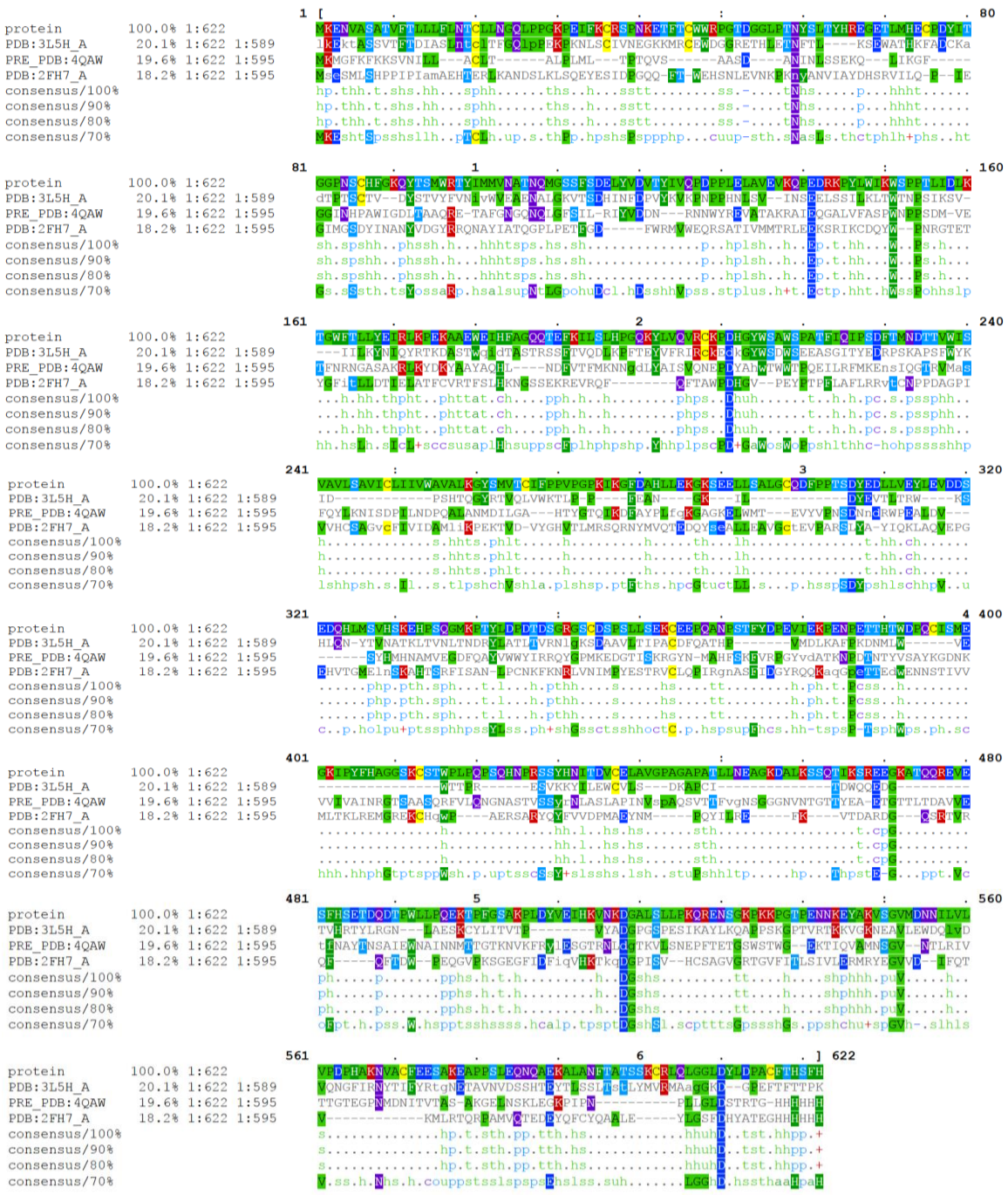

Figure 8: Sequence alignments of PRAP and homologs sequences obtained by pairwise algorithm. Residues are colored based on their properties.

electrophoresis (BioRad, USA), with the modification that samples, gels and running buffers were lacking SDS. The gels contained Acrylamide/Bis (30% T, 2.67% C) (Acrylamide: bis-acrylamide = 29.2:0.8) and 10% glycerol. The gel was run in buffer containing Tris (24 mM) and glycine (194 mM) at room temperature. Five microletre of the marker loaded in the first well with the samples each run. After completing the electrophoretic run, protein bands were visualized by staining with Coomassie Brilliant Blue G-250 and destained overnight with 7% (v/v) glacial acetic acid after documentation[41]. The molecular weight of the separated proteins was estimated in comparison to marker of standard molecular weights with regularly spaced bands ranging from 6.458 to 195.755 KDa. The native gels were also stained for lipid with Sudan Black B (SBB)[42].

Electrophoretic localization of in-gel enzyme activity

The non-denaturing gel was stained for electrophoretic POX pattern using benzidine stain prepared according to method described by Rescigno *et al.*[43]. It was stained for electrophoretic CAT pattern according to method of Siciliano and Shaw[44]. The native gel was processed for localization of in-gel EST

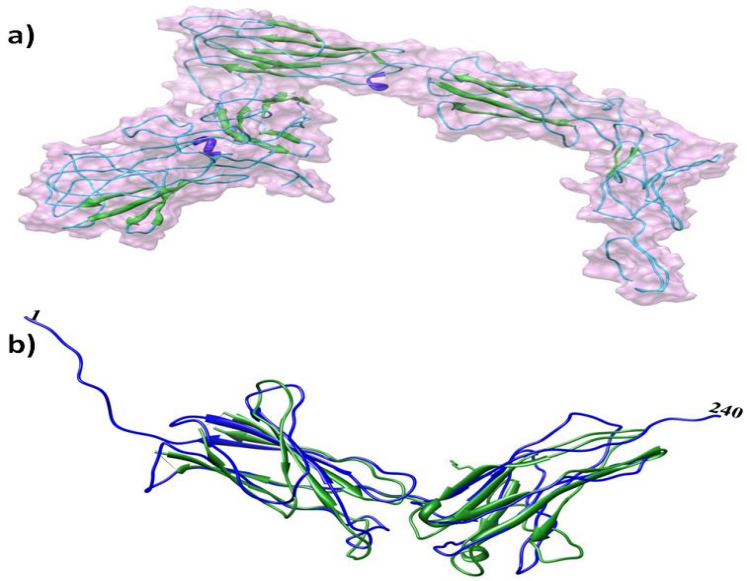

Figure 9: (a) Model of Prolactin receptor specific protein (PRAP). Domains are characterized by coil shape (cyan color), strand (green) and small helixes regions (blue), (b) Superimpose of PRAP model (residues 1-240, blue) with the crystal structure of prolactin receptor active domain (PDB: 4I18_C, green).

activity according to method suggested by Ahmad *et al.*[45] who postulated that the gel was incubated in reaction mixture containing α, β-naphthyl acetate (5.58 X 10^{-3} mM, pH 7.5) as substrates along with dye coupler Fast Blue RR at 25°C in dark. After developing the colored bands of EST activity, the reaction was stopped by fixing the gels in 7% glacial acetic acid for 30 min, followed by preserving the gel in 5% acetic acid prepared in 10% methanol.

Data analysis

All the native polyacrylamide gel plates were analyzed using Phoretix 1D pro software (Version 12.3). The similarity index (SI) was calculated according to equation suggested by Nei and Li[46] to compare all treated groups to control group.

Computational Methods

Comparative Protein Modeling

Comparative protein modeling uses previously solved structures as starting points, or templates. This is effective because it appears that although the number of actual proteins is vast, there is a limited set of tertiary structural motifs to which most proteins belong. It has been suggested that there are only around 2000 distinct protein folds in nature, though there are many millions of different proteins. Sequence-based methods for identifying protein homology compare sequences to find similarities that are unlikely to occur by chance. Essentially all methods employ some sort of scheme to judge amino acid substitutions, insertions and deletions. Based on the scoring scheme a query sequence is aligned to another sequence or to a profile that represents a set of sequences. In an alignment equivalent amino acids are set side-by-side so that insertions and deletions become apparent as shown in Fig. 1. The score of the sequence, which is used to detect homology, is directly related to the alignment. Profile-profile sequence-based homology detection was used. Sequences can be scored globally or locally. In the former case, the alignment is over the entire length of the sequences. From a biological point of view this is not always desired because related proteins may not have recognizable homology along their entire length. Proteins may for example share only one out of several domains. Local scoring aligns subsequences only and can be better for finding local similarities. It is also possible to align a global domain model locally to a sequence, (global/local scoring) or to align part of a domain model locally to a sequence (local/local scoring). Profile-profile methods are more sensitive[47] than both profile based and pair-wise methods[48,49].

Molecular Dynamics Simulations

Conceptually, molecular dynamics simulations are quite simple. In these simulations, we follow the trajectories of N particles interacting via a many-body potential $U(r_1, r_2, \ldots, r_N)$ using Newton's equation of motion[50]**:**

$$m_i \frac{d^2 r_i}{dr^2} = -\nabla_i U(r_1, \ldots\ldots, r_N) \quad ; \quad i = 1, \ldots\ldots, N$$

Where m_i and r_i denote the mass and position of the particle, and the force on it is given by the gradient of the potential U. Unlike in Brownian dynamics simulations, in which only the ions are simulated explicitly, in molecular dynamics all the atoms (ions, water, protein and lipid) can be included. At every time step, the potential function is recalculated using the new positions of the particles to determine their positions a short time later, and this process is iterated for a large number of steps until a statistically satisfactory data set is generated. The success of molecular dynamics simulations in capturing the dynamics of the real system hinges critically on how accurately the potential functions or force fields are selected. In the past two decades, numerous studies have been carried out to develop force fields for biomolecular applications, and these are incorporated into several user-friendly computer programs for simulation of biomolecular systems[51,52]. In these programs, the non-bonded interactions between atoms are represented by Coulomb and Lennard-Jones

Table 1: Electrophoretic pattern in the ovarian tissue showing the toxic effect on protein pattern in Pb-treated, Li_2CO_3-treated, Dox-treated, CCl_4-treated, CPA-treated and Irradiated groups of female rats.

Marker			Control				Toxic substances																	
							Pb-treated			Li_2CO_3-treated			Dox-treated			CCl_4-treated			CPA-treated			Irradiated		
Rm	Mwt	Ba %	Rm	Mwt	Ba %	Rm	Mwt	Ba %	Rm	Mwt	Ba %	Rm	Mwt	Ba %	Rm	Mwt	Ba %	Rm	Mwt	Ba %	Rm	Mwt	Ba %
0.11	195.70	25.99	0.06	234.46	14.64	0.06	234.46	13.40	0.08	223.39	12.79	0.09	215.64	15.95	0.09	214.53	14.28	0.08	218.96	12.30	0.09	211.21	11.15
0.24	107.10	14.72	0.12	192.28	6.41	0.13	183.16	13.94	0.13	182.02	9.15	0.13	183.16	6.89	0.14	176.34	5.68	0.15	170.66	8.39	0.14	176.34	5.59
0.32	59.20	9.30	0.18	145.95	6.66	0.18	145.95	5.93	0.18	149.29	1.22	0.18	148.18	6.31	0.19	144.84	6.31	0.20	134.92	9.65	0.19	139.32	5.25
0.37	41.20	9.53	0.23	116.57	6.15	0.23	117.63	4.89	0.23	116.57	10.76	0.22	119.77	4.48	0.22	119.77	5.22	0.28	83.11	9.28	0.24	109.19	4.98
0.47	27.50	9.50	0.27	89.86	6.20	0.27	91.83	9.43	0.27	87.91	3.98	0.25	100.90	5.76	0.28	83.11	7.32	0.34	51.55	7.71	0.27	87.91	3.97
0.56	20.50	9.67	0.34	53.53	11.22	0.33	58.46	8.28	0.35	49.06	5.99	0.30	73.06	7.22	0.35	46.73	9.50	0.40	35.45	9.64	0.30	71.32	3.77
0.76	15.10	12.22	0.39	37.66	8.55	0.40	34.37	8.56	0.41	33.41	8.21	0.35	49.67	5.92	0.40	35.45	5.43	0.46	28.45	1.88	0.35	49.67	5.87
0.97	6.40	9.08	0.44	30.07	11.50	0.44	29.67	6.62	0.45	29.29	3.69	0.43	31.44	7.39	0.44	29.67	5.64	0.49	25.82	3.60	0.41	34.12	5.48
—	—	—	0.48	26.62	2.85	0.48	27.00	5.05	0.48	27.13	5.01	0.48	27.25	4.97	0.48	26.62	6.36	0.53	22.82	4.83	0.45	29.04	5.12
—	—	—	0.64	16.95	17.72	0.65	16.78	15.62	0.51	24.73	2.05	0.53	22.69	6.16	0.65	16.81	12.93	0.66	16.68	19.82	0.50	25.41	4.73
—	—	—	0.97	6.48	8.12	0.97	6.40	8.29	0.57	19.70	4.70	0.64	16.95	13.02	0.74	15.40	16.01	0.78	14.65	6.59	0.54	21.66	4.75
—	—	—	—	—	—	—	—	—	0.64	17.06	10.73	0.73	15.63	8.95	0.97	6.40	5.33	0.97	6.27	6.32	0.63	17.22	16.75
—	—	—	—	—	—	—	—	—	0.72	15.76	15.65	0.97	6.56	6.97	—	—	—	—	—	—	0.73	15.55	4.70
—	—	—	—	—	—	—	—	—	0.98	6.21	6.07	—	—	—	—	—	—	—	—	—	0.78	14.48	8.50
—	—	—	—	—	—	—	—	—	—	—	—	—	—	—	—	—	—	—	—	—	0.82	13.26	4.43
—	—	—	—	—	—	—	—	—	—	—	—	—	—	—	—	—	—	—	—	—	0.96	6.80	4.95

Rm: Relative Mobility, Mwt: Molecular Weight, Ba %: Band Percent.
In each lane, arrangement of the bands is not correlated to arrangement of the bands in the other lanes.

potentials. Pairwise interactions are used for all the atoms in the system, and the potential parameters are determined empirically from spectroscopic data and fits to bulk properties. Most atoms in the system are also covalently bonded to other atoms, and these bonds are represented in molecular dynamics by a set of force parameters. For a geometry in Figure 2 the bonds will typically involve the separation $r_{12} = |r_1 - r_2|$ between adjacent pairs of atoms in a molecular framework. The bend angles θ_{123} is between successive bond vectors (r2 − r1) and (r2 − r3). Usually this bending term is taken to be quadratic in the angular displacement from the equilibrium value. The torsion angles Φ_{1234} are defined in terms of three connected bonds, hence four atomic coordinates:

$$\cos\phi_{1234} = -\hat{n}_{123} \cdot \hat{n}_{234}$$

Where $n_{123} = r_{12} \times r_{23}$, $n_{234} = r_{23} \times r_{34}$.
The normal unit defined by each pair of bonds. Usually the torsional potential involves an expansion in periodic functions[53].

RESULTS

The native electrophoretic protein pattern in the healthy ovarian tissue produced 11 bands with Rms ranged between 0.06 – 0.97 (Mwts 6.48 – 234.46 KDa and Ba % values 2.85 – 17.72). As compiled in Table 1 and illustrated in Fig. 3a, there were 3 common bands appeared in all groups with Rms 0.48, 0.64 and 0.97 (Mwts 26.62, 16.95 and 6.48 and Ba % values 2.85, 17.72 and 8.12 respectively). The 3rd, 4th and 8th bands (Rms 0.18, 0.23 and 0.44, Mwts 145.95, 116.57 and 30.07 and Ba % values 6.66, 6.15 and 11.50) were considered as common bands in all groups except CPA-treated group. One characteristic bands appeared in the Li_2CO_3-treated group with Rm 0.57 (Mwt 19.70 and Ba % 4.70) and another one noticed in irradiated group with Rm 0.82 (Mwt 13.26 KDa and Ba % 4.43). In the Li_2CO_3-treated group, the 1st and 7th bands deviated to be appeared with Rms 0.08 and 0.41 (Mwts 223.39 and 33.41 and Ba % values 12.79 and 8.21). In addition, there were 2 abnormal bands appeared with Rms 0.57 and 0.72 (Mwts 19.70 and 15.76 and Ba % values 4.70 and 15.65). Moreover, there was quantitative mutation represented by decreasing Ba % of the 3rd, 5th, 6th and 8th bands (Rms 0.18, 0.27, 0.35 and 0.45, Mwts 149.29, 87.91, 49.06 and 29.29 and Ba % values 1.22, 3.98, 5.99 and 3.69) respectively. Administration of CCl_4 showed the lowest effect on the native protein pattern. In the Pb-treated group, there was quantitative alterations represented by decreasing Ba % of the 8th band (Rm 0.44, Mwt 29.67 KDa and Ba % 5.64) and increasing Ba % of the 9th band (Rm 0.48, Mwt 26.62 KDa and Ba % 6.36). From the SI values,

Table 2: Electrophoretic pattern in the ovarian tissue showing the toxic effect on lipoprotein pattern in Pb-treated, Li_2CO_3-treated, Dox-treated, CCl_4-treated, CPA-treated and Irradiated groups of female rats.

Control		Toxic substances											
		Pb-treated		Li_2CO_3-treated		Dox-treated		CCl_4-treated		CPA-treated		Irradiated	
Rm	Ba %	Rm	Ba %	Rm	Ba %	Rm	Ba %	Rm	Ba %	Rm	Ba %	Rm	Ba %
0.04	70.57	0.04	35.78	0.05	11.37	0.11	100	0.11	100	0.04	11.09	0.04	7.34
0.46	16.66	0.22	64.22	0.23	88.63	—	—	—	—	0.1	33.5	0.08	9.3
0.59	12.77	—	—	—	—	—	—	—	—	0.25	55.41	0.14	83.37

Rm: Relative Mobility, Ba %: Band Percent.
Arrangement of the bands in each lane is not correlated with the bands in the other lanes.

Table 3: Electrophoretic pattern in the ovarian tissue showing the toxic effect on CAT pattern in Pb-treated, Li_2CO_3-treated, Dox-treated, CCl_4-treated, CPA-treated and Irradiated groups of female rats.

Control		Toxic substances											
		Pb-treated		Li_2CO_3-treated		Dox-treated		CCl_4-treated		CPA-treated		Irradiated	
Rm	Ba %	Rm	Ba %	Rm	Ba %	Rm	Ba %	Rm	Ba %	Rm	Ba %	Rm	Ba %
0.06	25.63	0.05	26.05	0.06	22.8	0.05	23.26	0.06	29.83	0.05	37.29	0.06	17.46
0.26	20.76	0.26	21.54	0.26	20.25	0.25	20.14	0.24	44.42	0.18	36.69	0.19	15.78
0.48	34.62	0.48	32.89	0.34	19.43	0.32	26.64	0.96	25.75	0.96	26.02	0.97	66.77
0.98	18.99	0.97	19.52	0.42	20.46	0.97	29.96	—	—	—	—	—	—
—	—	—	—	0.97	17.06	—	—	—	—	—	—	—	—

Rm: Relative Mobility, Ba %: Band Percent.
In each lane, arrangement of the bands is not correlated to arrangement of the bands in the other lanes.

Table 4: Electrophoretic pattern in the ovarian tissue showing the toxic effect on POX pattern in Pb-treated, Li_2CO_3-treated, Dox-treated, CCl_4-treated, CPA-treated and Irradiated groups of female rats.

Control		Toxic substances											
		Pb-treated		Li_2CO_3-treated		Dox-treated		CCl_4-treated		CPA-treated		Irradiated	
Rm	Ba %	Rm	Ba %	Rm	Ba %	Rm	Ba %	Rm	Ba %	Rm	Ba %	Rm	Ba %
0.32	0.57	0.61	1.66	0.38	12.66	0.19	16.36	0.48	17.09	0.14	13.22	0.32	38.92
0.6	40.48	0.84	98.34	0.47	19.88	0.33	19.22	0.59	0.98	0.25	10.53	0.59	0.57
0.85	58.95	—	—	0.6	1.48	0.5	11.61	0.82	81.93	0.35	10.91	0.78	33.48
—	—	—	—	0.85	65.99	0.6	0.5	—	—	0.44	14.82	0.83	27.04
—	—	—	—	—	—	0.84	52.32	—	—	0.59	0.76	—	—
—	—	—	—	—	—	—	—	—	—	0.82	49.76	—	—

Rm: Relative Mobility, Ba %: Band Percent.
Arrangement of the bands at each lane is not correlated with the bands in the other lanes.

it was noticed that the lowest SI value (0.52) was recorded with CPA-treated group and the highest SI value (0.91) was recorded with Pb-treated group (Fig. 3b). In the healthy ovarian tissue, lipoprotein pattern produced 3 bands with Rms 0.04, 0.46 and 0.59 (Ba % 70.57, 16.66 and 12.77) respectively. There were no common bands. The 1st band was considered as common band in all the groups except Dox-treated and CPA-treated groups (Table 2 and Fig. 4a). In the Pb-treated and Li_2CO_3-treated groups, the qualitative and quantitaive alterations occurred with the same degree. In Pb-treated group, these disturbances were represented by disappearance of 2 normal bands with appearance of one abnormal band with Rfm0.22 (Ba % 64.22). In addition, the quantitative mutation occured by decreasing Ba % of the 1st band (Rm 0.04 and Ba % 35.78). In Li_2CO_3-treated group, the abnormal band was appeared with Rm 0.23 (Ba % 88.63) and the quantitative mutation represented by decreasing Ba % of the 1st band (Rm 0.05 and Ba % 11.37). In the Dox-treated and CPA-treated groups, the alteration occurred qualitatively with the same degree by disappearance of the normal bands with appearance of one abnormal band with Rm 0.11 (Ba % 100.00). In the CCl_4-treated and irradiated groups, the alteration occurred quanlitatively with the same degree by disappearance of 2 normal bands with appearance of 2 abnormal band with Rms 0.10 and 0.25 (Ba % 33.50 and 55.41) as in CCl_4-treated group and with Rms 0.080 and 0.14 (Ba % 9.30 and 83.37) as in the irradiated group. As illustrated in Fig. 4b, the lowest SI value (0.33) was recorded with CCl_4-treated and Irradiated groups. The highest SI (0.40) was noticed with Pb-treated and Li_2CO_3-treated groups. Moreover, in the Dox-treated and CPA-treated groups, it was observed that all the bands were not matched with all bands in the other groups. The electrophoretic CAT pattern showed that 4 types of the enzyme were noticed in healthy ovarian tissue with Rms 0.06, 0.26, 0.48 and 0.98 (Ba % values 25.63, 20.76, 34.62 and 18.99) respectively. There were 2 common bands

Table 5: Electrophoretic pattern in the ovarian tissue showing the toxic effect on EST pattern in Pb-treated, Li_2CO_3-treated, Dox-treated, CCl_4-treated, CPA-treated and Irradiated groups of female rats.

Control		Toxic substances											
		Pb-treated		Li_2CO_3-treated		Dox-treated		CCl_4-treated		CPA-treated		Irradiated	
Rm	Ba %	Rm	Ba %	Rm	Ba %	Rm	Ba %	Rm	Ba %	Rm	Ba %	Rm	Ba %
0.24	54.11	0.15	38.65	0.25	44.12	0.25	54.24	0.27	73.67	0.39	78.08	0.26	37.68
0.38	23.65	0.24	12.36	0.78	55.88	0.36	26.05	0.37	26.33	0.77	21.92	0.38	16.95
0.76	22.24	0.36	27.86	—	—	0.77	19.71	—	—	—	—	0.78	45.37
—	—	0.75	21.13	—	—	—	—	—	—	—	—	—	—

Rm: Relative Mobility, Ba %: Band Percent.
In each lane, arrangement of the bands is not correlated to arrangement of the bands in the other lanes.

appeared with Rms 0.06 and 0.98 (Ba % 25.63 and 18.99). As compared to control, no qualitative or quantitative alterations observed in Pb-treated group. In the Li_2CO_3-treated group, the qualitative alterations represented by disappearance of one normal type with appearance of 2 abnormal types with Rms 0.34 and 0.42 (Ba % 19.43 and 20.46). In the Dox-treated group, the qualitative mutation was represented by deviation of the 3rd normal type to be appeared with Rm 0.32 (Ba % 26.64). While in the CCl_4-treated group, the mutation was represented by disappearance of the 3rd type of the enzyme completely. The electrophoretic alterations were identical in the CPA-treated and Irradiated groups. These alterations were represented by disappearance of the 3rd type with deviation of the 2nd type of the enzyme to be appeared with Rm 0.18 (Ba % 36.69). On the other hand, there was quantitative alterations occurred in Ba % of the 1st and 4th types of the enzyme in both groups (Table 3 and Fig. 5a). As illustrated in the Fig. 5b, the lowest SI value (0.57) was observed with CPA-treated and Irradiated groups. The Pb-treated group was completely identical to control group in number and arrangement of the bands (the highest SI value 1.0). Electrophoretic POX pattern showed that 3 types of this enzyme were produced in control ovarian tissue with Rms 0.32, 0.60 and 0.85 (Ba % values 0.57, 40.48 and 58.95) respectively. There were no common bands. As revealed in Table 4 and illustrated in Fig. 6a, the 3rd type of the enzyme (Rm 0.85 and Ba % 58.95) was considered as common band in all groups except Li_2CO_3-treated and Dox-treated groups. In the Pb-treated group, the qualitative alteration was represented by disappearance of the 1st type. The quantitative mutation was represented by decreasing Ba % of the 2nd type (Rm 0.61 and Ba % 1.66) and increasing Ba % of the 3rd type (Rm 0.84 and Ba % 98.34). The abnormalities occurred in the Li_2CO_3-treated group were represented qualitatively by disappearance of the 1st type with appearance of 2 abnormal bands (Rms 0.38, 0.47, Ba % values 12.66 and 19.88). This was in addition to the quantitative mutation which was represented by decreasing Ba % of the 2nd type (Rm 0.60 and Ba % 1.48). In Dox-treated group, There were alterations were represented qualitatively by appearance of 2 abnormal bands with Rms 0.19 and 0.50 (Ba % 16.36 and 11.61). Also, these alterations were represented quantitatively by increasing Ba % of the 1st type (Rm 0.33 and Ba % 19.22) and decreasing Ba % of the 2nd type (Rm 0.60 and Ba % 0.50). In CCl_4-treated group, the alterations were represented by disappearance of the 1st type with appearance of one abnormal band (Rm 0.48 and Ba % 17.09). Moreover, the 3rd type deviated to be appeared with Rm 0.82 (Ba % 81.93). The quantitative alteration was represented by decreasing Ba % of the 2nd type (Rm 0.59 and Ba % 0.98) and increasing Ba % of the 3rd type (Rm 0.82 and Ba % 81.93). In CPA-treated group, the qualitative mutation was represented by appearance of 3 abnormal bands with Rms 0.14, 0.25 and 0.44 (Ba % values 13.22, 10.53 and 14.82) respectively. This was in association with deviation of the 1st and 3rd types to be appeared with Rms 0.35 and 0.82 (Ba % 10.91 and 49.76). The mutation occurred quantitatively by increasing Ba % of the 1st type (Rm 0.35 and Ba % 10.91) and decreasing Ba % of the 2nd type of the enzyme (Rm 0.59 and Ba % 0.76). In irradiated group, the mutation occurred qualitatively by appearance of one abnormal band (Rm 0.78 and Ba % 33.48) and quantitatively by increasing Ba % of the 1st type (Rm 0.32 and Ba % 38.92) and decreasing Ba % of the 2nd and 3rd types of the enzyme (Rms 0.59, 0.83, Ba % values 0.57 and 27.04). The SI values were ranged between 0.22 – 0.86. The lowest SI value (0.22) was recorded with CPA-treated group and the hightest value (0.86) was noticed with irradiated group (Fig. 6b). As recorded in Table 5 and illustrated in Fig. 7a, the electrophoretic EST pattern showed that 3 types of this enzyme produced in healthy ovarian tissue with Rms 0.24, 0.38 and 0.76 (Ba % 54.11, 23.65 and 22.24) respectively. There were no common bands. The 3rd type was considered as common band in all groups except Pb-treated and CCl_4-treated groups. In the Pb-treated group, the qualitative mutation represented by appearance of one abnormal characteristic band with Rm 0.15 (Ba % 38.65). This was in addition to the quantitative mutation represented by decreasing Ba % of the 1st normal type (Rm 0.24 and Ba % 12.36). Lithium caused mutation represented qualitatively by disappearance of the 2nd normal type and quantitatively by increasing Ba % of the 3rd type of the enzyme (Rm 0.78 and Ba % 55.88). There were no qualitative or quantitative alterations in the Dox-treated group. While in the irradiated group, the alteration occurred quantitatively by decreasing Ba % of the 1st type (Rm 0.26 and Ba % 37.68) and increasing Ba % of the 3rd type of the enzyme (Rm 0.78 and Ba % 45.37). In the CCl_4-treated group, the alterations were represented qualitatively by disappearance of the 3rd normal type with deviation of the 1st type to be appeared with Rm 0.27 (Ba

% 73.67). This was in addition to the quantitative mutation occurred by increasing Ba % of the 1st type of the enzyme (Rm 0.27 and Ba % 73.67). While in the CPA-treated group, the alteration was represented by disappearance of the 1st type with increasing Ba % of the 2nd type of the enzyme (Rm 0.39 and Ba % 78.08). The lowest SI value (0.29) was reported with the Pb-treated group and the highest SI value (0.80) was noticed with the Li_2CO_3-treated group. As revealed in the Fig. 7b, there was complete similarity between the Dox-treated and Irradiated groups and between CCl_4-treated and CPA-treated groups. Homology of PRAP was constructed by restraint-based comparative modeling using templates obtained from FASTA and BLAST databases [H. McWilliam H, W. Li, M. Uludag, S. Squizzato, Y. M. Park, N. Buso, A. P. Cowley, R. Lopez, Analysis Tool Web Services from the EMBL-EBI, Nucleic acids research 41 (Web Server issue): W597-600 (2013 Jul) - A. Morgulis, G. Coulouris, Y. Raytselis, T. L. Madden, R. Agarwala, A. A. Schäffer, "Database indexing for production MegaBLAST searches." Bioinformatics 15: 1757-1764 (2008)]. Templates were selected according to the similarity with the query sequence (with similarity percent of 21.0±2%). The model was construct using multiple alignment by means of restraint-based comparative modeling, using the X-ray crystallographic structures of Interleukin-6 receptor (PDB ID: 3l5h, and 3l5i), modular Xyn30D from Paenibacillus barcinonensis (PDB ID: 4qaw), and tyrosine-protein phosphatase S (PDB: 2fh7) as templates. [Y. Zhang. I-TASSER server for protein 3D structure prediction. BMC Bioinformatics, 9:40 (2008) - A. Roy, A. Kucukural, Y. Zhang. I-TASSER: a unified platform for automated protein structure and function prediction. Nature Protocols, vol 5, 725-738 (2010) - A. Roy, J. Yang, Y. Zhang. COFACTOR: an accurate comparative algorithm for structure-based protein function annotation. Nucleic Acids Research, 40, W471-W477 (2012)]. Pairwise alignment between PRAP and homologs sequences is presented in Fig. 8. It is obvious that the global alignment shows good agreement between the sequences. Using these alignment results, novel model of PRAP protein was constructed and minimized. As illustrated in Fig. 9a, the data show the constructed model where it can be seen that it consists of coil secondary structure. The constructed model was tested by superimposing the receptor domain (residues 1 - 240) with a recently released prolactin receptor complex domain (PDB: 4I18_C) [10.2210/pdb4i18/pdb] where the calculated root mean square (RMS) was only 3.62 Å (see Fig. 9b).

DISCUSSION

Proteins are the most susceptible macromolecules to be oxidized than others. This depends on the relative content of oxidation-sensitive amino acid residues[54]. Polyacrylamide gel electrophoresis was used for separation and identifying of different proteins and isoenzymes. During the present study, this technique was used to show the deleterious effect of various toxic factors on the different intracellular macromolecules inside the ovarian tissue in rats. During the present study, lithium and lead caused alterations in the native protein pattern detected electrophoretically in the ovarian tissue. This may be due to the presence of specific metal-binding sites[55]. The metal-catalysed oxidation is considered as the most common mechanism which is responsible for protein oxidation. During this mechanism, these metal ions bind to metal binding sites within proteins and react with H_2O_2 to generate hydroxyl radicals that attack neighboring amino acid residues[56,57]. The variations in electrophoretic mobility may be attributed to effect of the free radicals on integrity of the polypeptide chain in the protein molecule. Subsequently, this leads to sulfhydral-mediated cross linking of the labile amino acids and hence fragmentation of the polypeptide chains[58]. According to results of the current study, it was found that all the toxic factors selected to be under this study caused electrophoretic alterations in the native protein pattern. This may refer to generation of the free radicals which exhibit modifications in the amino acids through their direct reaction with side chains. It was found previously that the amino acids which contain aromatic side chain groups are the most sensitive to the free radicals attack and these amino acids form carbonyl products irreversibly during the oxidation reaction[59]. Lipoproteins carry all types of lipids, but in different proportions. The density is directly proportional to the protein content and inversely proportional to the lipid content[60]. For this reason, the alterations in the lipoprotein pattern may refer to the changes in the protein portion. The variations in isoenzymes seem to be good markers of the physiological changes in granulosa cells in the ovary[61]. During the current experimental study, it was found that all the toxic factors caused disturbances in the electrophoretic isoenzymes. This was in accordance with El-Zayat[62] who emphasized the changes in the fractional activity of different isoenzymes seemed to be correlated with changes in the rate of protein expression secondary to DNA damage initiated by free radicals. In addition, further studies confirmed that the differences in the electrophoretic isoenzymes may be attributed due to effect of the free radicals which cause oxidation at level of the nucleic acids. This leads to the formation of various molecular lesions including oxidized bases (purines and pyrimidines), abasic sites (apurinic/apyrimidinic sites) and DNA single- and/or double-strand breaks. Guanine is the most DNA base which is susceptible to be oxidized[63]. Hydroxyl radicals react with pyrimidines (thymine and cytosine) at positions 5 or 6 of the ring producing several lesions[64]. It was found that the follicular fluid microenvironment contains leukocytes, macrophages and cytokines which are considered as sources of ROS[65]. Due to data of the present study, it was found that there were severe alterations in CAT and POX in the ovarian tissue. This might be occurred due to effect of the free radicals generated as a result of the exposure to these toxic factors. These free radicals caused several molecular alterations involving directly in accumulation of genetic changes and depletion of antioxidant enzymes[66]. Moreover, Peltola *et al*. (1994)[67] reported that the disturbances in electrophoretic CAT isoenzymes in the ovarian tissue might be related to

oxidative stress and attack of the free radicals to protein portion of the native enzymes. On the other hand, it is well known that the chemotherapeutic drugs caused depletion of GSH[23]. The alterations in the electrophoretic POX pattern may be caused due to depletion in the level of reduced GSH[68]. This leads to elevation of H_2O_2 and hence generation of the free radicals[69]. The oocytes and granulosa cells of secondary follicles are rich in EST enzyme[70]. The alterations in the electrophoretic EST pattern may occur due to expression of various markers of oxidative stress[71]. The cellular endocytosis occurred as a result of enhancing expression of the PRLR and stimulating phosphorylation of the PRLR at Ser-349. Moreover, degradation of the cell occurred through reducing PRLR expression[72]. It was demonstrated previously that down-regulation of the receptor occurred under control of the hormones which decrease expression of the genes which are responsible for synthesis of these receptors and hence reducing the receptors affinity[73]. Understanding structure of PRAP is vital because it is included in various metabolic reactions as well as interaction with certain hormones and it was found to exist in certain tumor cell reactions [Jan van Agthoven, Chi Zhang, Estelle Tallet, Bertrand Raynal, Sylviane Hoos, Bruno Baron, Patrick England, Vincent Goffin, Isabelle Broutin, Journal of Molecular Biology, 404, 112 – 126 (2013)]. During the current study, it was postulated that PRAP is expected to be very flexible protein and might be less stable as compared to the Dual specificity testis-specific protein kinase 1 which is predominantly expressed in testicular germ cells and may play an important role in spermatogenesis. This may refer to the large amount of loops on it that was resulted from the 3D homology modeling.

CONFLICTS OF INTEREST

There are none declared conflicts of interest by authors

REFERENCES

1. Yu Q, Rengel Z. Drought and salinity differentially influence activities of superoxide dismutases in narrow-leafed lupins. Plant Sci 1999; 142 (1): 1-11.
2. Alscher RG, Erturk N, Heath LS. Role of superoxide dismutases (SODs) in controlling oxidative stress in plants. J Exp Bot 2002; 53 (372):1331-1341.
3. Baek KH, Skinner DJ. Alteration of antioxidant enzyme gene expression during cold acclimation of near-isogenic wheat lines. Plant Sci 2003; 165 (6):1221-1227.
4. Mauro F, Van Eycken N, Challou P, Lucas M, L'Oiseau M. Characterization of new maize chloroplastic copper/zinc superoxide dismutase isoforms by high resolution native two-dimensional ployacrylamide gel electrophoresis. Identification of chilling responsive chloroplastic superoxide dismutase isoforms. Physiol Plant 2005; 124 (3):323-335.
5. Khan N, Naqvi FN. Agro-biochemical Traits of Wheat Genotypes Under Irrigated and Non-Irrigated Conditions. Cereal Research Communications 2013; 41 (2) :243-254.
6. Scandalios JG. Oxygen stress and superoxide dismutases. Plant Physiol 1993; 101 (1): 7-12.
7. Harrison JF, Hollensworth SB, Spitz DR, Copeland WC, Wilson GL, LeDoux SP. Oxidative stress-induced apoptosis in neurons correlates with mitochondrial DNA base excision repair pathway imbalance. Nucleic Acids Research 2005; 33 (14): 4660–4671.
8. Shakeel S, Simeen M. Pretreatment effect of salicylic acid on protein and hydrolytic enzymes in salt stressed mung bean seedlings. Asian J Agricultural Sciences 2012; 4 (2): 122-25.
9. Deavall DG, Martin EA, Horner JM, Roberts R. Drug-Induced Oxidative Stress and Toxicity. Journal of Toxicology 2012; Article ID 645460, 13 pages.
10. Nunes MA, Viel TA, Buck HS. Microdose lithium treatment stabilized cognitive impairment in patients with Alzheimer's disease. Curr Alzheimer Res 2013; 10(1):104-7.
11. Griffiths JJ, Zarate CA, Rasimas JJ. Existing and novel biological therapeutics in suicide prevention. Am J Prev Med 2014; 47(3 Suppl 2): S195-203.
12. Kushchayeva Y, Jensen K, Burman KD, Vasko V. Repositioning therapy for thyroid cancer: new insights on established medications. Endocr Relat Cancer 2014; 21(3): R183-94.
13. Jana D, Nandi D, Maiti R, Ghosh D. Effect of human chorionic gonadotrophin coadministration on the activities of ovarian Delta5-3beta-hydroxysteroid dehydrogenase, and 17beta-hydroxysteroid dehydrogenase, and ovarian and uterine histology in lithium chloride-treated albino rats. Reprod Toxicol 2001; 15(2):215-9.
14. Khodadadi M, Pirsaraei ZA. Disrupting effects of lithium chloride in the rat ovary: Involves impaired formation and function of corpus luteum. Middle East Fertility Society Journal 2013; 18 (1): 18–23.
15. Waseem N, Butt SA, Hamid S. Amelioration of lead induced changes in ovary of mice, by garlic extract. J Pak Med Assoc 2014; 64(7):798-801.
16. Chemaitilly W, Mertens AC, Mitby P, Whitton J, Stovall M, Yasui Y, Robison LL, Sklar CA. Acute ovarian failure in the childhood cancer survivor study. J. Clin. Endocrinol. Metab 2006; 91 (5) :1723–1728.
17. Seski JC, Edwards CL, Gershenson DM, Copeland LJ. Doxorubicin and cyclophosphamide chemotherapy for disseminated endometrial cancer. Obstet Gynecol 1981; 58(1):88-91.
18. Meirow D, Lewis H, Nugent D, Epstein M. Subclinical depletion of primordial follicular reserve in mice treated with cyclophosphamide: clinical importance and proposed accurate investigative tool. Hum Reprod 1999; 14 (7) :1903-1907.
19. Fortune JM, Osheroff N. Topoisomerase II as a target for anticancer drugs: when enzymes stop being nice. Progress in Nucleic Acid Research and Molecular Biology 2000; 64: 221–253.
20. Sardao VA, Oliveira PJ, Holy J, Oliveira CR, Wallace KB. Morphological alterations induced by doxorubicin on H9c2 myoblasts: nuclear, mitochondrial, and

cytoskeletal targets. Cell Biol Toxicol 2009; 25 (3): 227-243.
21. Ben-Aharon I, Bar-Joseph H, Tzarfaty G, Kuchinsky L, Rizel S, Stemmer SM, Shalgi R. Doxorubicin-induced ovarian toxicity. Reproductive Biology and Endocrinology 2010; 8:20
22. Tomao F, Spinelli GP, Panici PB, Frati L, Tomao S. Ovarian function, reproduction and strategies for fertility preservation after breast cancer. Critical Reviews in Oncology/Hematology 2010; 76 (1): 1–12.
23. Lopez SG, Luderer U. Effects of cyclophosphamide and buthionine sulfoximine on ovarian glutathione and apoptosis. Free Radic Biol Med 2004; 36(11):1366-77.
24. Hanoux V, Pairault C, Bakalska M, Habert R, Livera G. Caspase-2 involvement during ionizing radiation-induced oocyte death in the mouse ovary. Cell Death Differ 2007; 14 (4) :671–681.
25. Ben-Jonathan N, LaPensee CR, LaPensee EW. What can we learn from rodents about prolactin in humans?. Endocr Rev 2008; 29 (1) :1–41.
26. Huang YM, Shi ZD, Tian YB. Research progress in effect of prolactin on promotion of follicles development in poultry. J Zhongkai Univ Agric Technol 2008; 21:66–70.
27. Bu G, Wang CY, Cai G, Leung FC, Xu M, Wang H, Huang G, Li J, Wang Y. Molecular characterization of prolactin receptor (cPRLR) gene in chickens: Gene structure, tissue expression, promoter analysis, and its interaction with chicken prolactin (cPRL) and prolactin-like protein (cPRL-L). Mol Cell Endocrinol 2013; 370(1-2):149-62.
28. Luo A, Yang S, Shen W. Expression of ovarian prolactin receptor mRNA during follicular development and ovulation in the mouse. Chin J Histochem Cytochem 2010; 19:390–3.
29. Kelly PA, Binart N, Lucas B, Bouchard B, Goffin V. Implications of multiple phenotypes observed in prolactin receptor knockout mice. Front Neuroendocrinol 2001; 22 (2):140–5.
30. Kiapekou E, Loutradis D, Mastorakos G, Bletsa R, Beretsos P, Zapanti E, Drakakis P, Antsaklis A, Kiessling AA. Effect of PRL on in vitro follicle growth, in vitro oocyte maturation, fertilization and early embryonic development in mice. Cloning Stem Cells 2009; 11 (2) :293–300.
31. Xie Y-L, Hassan SA, Qazi AM, Tsai-Morris CH, Dufau ML. Intramolecular disulfide bonds of the prolactin receptor short form are required for its inhibitory action on the function of the long form of the receptor. Molecular and Cellular Biology 2009; 29 (10): 2546–2555.
32. Elgawish RA, Abdelrazek HMA. Effects of lead acetate on testicular function and caspase-3 expression with respect to the protective effect of cinnamon in albino rats. Toxicology Reports 2014; 1: 795–801.
33. Hosseini E, Dalaeli Z. The Perinatal Effects of Lithium Carbonate on Hypothalamic-Pituitary-Gonadal in Adult Female Wistar Rats. J Fasa Univ Med Sci 2015; 5(3): 397-404.
34. Hozayen WG. Effect of Hesperidin and Rutin On Doxorubicin Induced Testicular Toxicity in Male Rats. International Journal of Food and Nutrition Science 2012; 1 (1): 31 – 42.
35. Eidi A, Mortazavi P, Tehrani ME, Rohani AH, Safi S. Hepatoprotective effects of pantothenic acid on carbon tetrachloride-induced toxicity in rats. EXCLI Journal 2012; 11: 748-759.
36. Kanth MA, Kaur P, Ahmad B, Sharma S. Histological effect of anticancer drug cyclophosphamide (CP) on testis of *Rattus rattus*. Indo American Journal of Pharm Research 2014; 4(05):2645-2649.
37. Abulyazid I, Abdalla MS, Sharada HM, Abd El Kader MA, Kamel WM. Protective Effect of Salicin Isolated from Egyptian Willow Leaves *(Salix subserrata)* against Gamma-Radiation-Induced Electrophoretic and Molecular Changes in Epididymal Tissue in Rats. International Journal of Recent Scientific Research 2015; 6(6): 4421-4435.
38. Elshawi OE, Nabil AI, Mahmoud MF. Testicular damages mediated by oxidative stress in swiss albino rats exposed to lead acetate and gamma rays co-toxicity the possible protective role of taurine. J Appl Environ Biol Sci 2014; 4(8)279-291.
39. Bradford MM. (1976). A rapid and sensitive method for the quantitation of microgram quantities of protein utilizing the principle of protein-dye binding. Anal Biochem 1976; 72 (1-2): 248-254.
40. Laemmli UK. Cleavage of structural proteins during the assembly of the head of Bacteriophage T4. Nature 1970; 227: 680-685.
41. Darwesh OM, Moawad H, Barakat OS, Abd El-Rahim WM. Bioremediation of Textile Reactive Blue Azo Dye Residues using Nanobiotechnology Approaches. Research Journal of Pharmaceutical, Biological and Chemical Sciences 2015; 6(1): 1202- 1211.
42. Subramaniam HN, Chaubal KA. Evaluation of intracellular lipids by standardized staining with a Sudan black B fraction. J Biochem Biophys Methods 1990; 21(1):9-16.
43. Rescigno A, Sanjust E, Montanari L, Sollai F, Soddu G, Rinaldi AC, Oliva S, Rinaldi A. Detection of laccase, peroxidase and polyphenol oxidase on a single polyacrylamide gel electrophoresis. Anal Lett 1997; 30(12): 2211-2220.
44. Siciliano MJ, Shaw CR. Separation and visualization of enzymes on gels, in Chromatographic and Electrophoretic Techniques, Vol. 2, Zone Electrophoresis, Smith, I., Ed., Heinemann, London 1976; p. 185.
45. Ahmad A, Maheshwari V, Ahmad A, Saleem R, Ahmad R. Observation of esterase-like-albumin activity during N'- nitrosodimethyl amine induced hepatic fibrosis in a mammalian model. Maced J Med Sci 2012; 5(1): 55–61.
46. Nei M, Li WS. Mathematical model for studing genetic variation in terms of restriction endonuclease. Proc Natl Acad Sci USA 1979; 76 (10): 5269 – 5273.
47. Soding J. Protein homology detection by HMM-HMM comparison. Bioinformatics 2005; 21(7): 951-60.

48. Park J, Karplus K, Barrett C, Hughey R, Haussler D, Hurbbard T, Chothia C. Sequence comparisons using multiple sequences detect three times as many remote homologues as pairwise methods. J Mol Biol 1998; 284: 1201-10.
49. Lindahl E, Elofsson A. Identification of related proteins on family, superfamily and fold level. J Mol Biol 2000 ; 295(3):613-25.
50. Hermans J, Berendsen HJC, van Gunsteren WF, Postma JPM. A consistent empirical potential for water–protein interactions. Biopolymers 1984; 23 (8): 1513-1518.
51. Weiner SJ, Kollman PA, Case DA, Singh UC, Ghio C, Alagona G, Profeta S, Weiner P. A new force field for molecular mechanical simulation of nucleic acids and proteins. J Am Chem Soc 1984; 106 (3):765–784.
52. Kale´ L, Skeel R, Bhandarkar M, Brunner R, Gursoy A, Krawetz N, Phillips J, Shinozaki A, Varadarajan K, Schulten K. NAMD2: Greater scalability for parallel molecular dynamics. J Comput Phys 1999; 151: 283-312.
53. Price SL. Toward more accurate model of intermolecular potentials for organic molecules. Rev Comput Chem 2000; 14: 225-89.
54. Östman A, Frijhoff J, Sandin Å, Böhmer F-D. Regulation of protein tyrosine phosphatases by reversible oxidation. Journal of Biochemistry 2011; 150 (4): 345–356.
55. Avery SV. Molecular targets of oxidative stress. Biochemical Journal 2011; 434 (2): 201–210.
56. Stadtman ER, Levine RL. Free radical-mediated oxidation of free amino acids and amino acid residues in proteins. Amino Acids 2003; 25 (3-4) 207–218.
57. Cecarini V, Gee J, Fioretti E, Amici M, Angeletti M, Eleuteri AM, Keller JN. Protein oxidation and cellular homeostasis: Emphasis on metabolism. Biochim Biophys Acta 2007; 1773(2):93-104.
58. Bedwell S, Dean RT, Jessup W. The action of defined oxygen centered free radicals on human low-density lipoprotein. Biochem J 1989; 262: 707-712.
59. Shringarpure R, Grune T, Mehlhase J, Davies KJA. Ubiquitin conjugation is not required for the degradation of oxidized proteins by proteasome. The Journal of Biological Chemistry 2003; 278 (1): 311–318.
60. Bass KM, Newschaffer CJ, Klag MJ, Bush TL. Plasma lipoprotein levels as predictors of cardiovascular death in women. Arch Intern Med 1993; 153(19): 2209-2216.
61. Beckmans L, Bergman S, Bjersing L. Esterase isozymes in granulosa cells of porcine ovarian follicles and corpora lutea. Hereditas 1975; 79(2): 303 – 4.
62. El-Zayat EM. Isoenzyme Pattern and Activity in Oxidative Stress-Induced Hepatocarcinogenesis: The Protective Role of Selenium and Vitamin E. Research Journal of Medicine and Medical Sciences 2007; 2(2): 62-71.
63. Neeley WL, Essigmann JM. Mechanisms of formation, genotoxicity, and mutation of guanine oxidation products. Chemical Research in Toxicology 2006; 19 (4): 491–505.
64. Purmal AA, Kow YW, Wallace SS. Major oxidative products of cytosine, 5-hydroxycytosine and 5-hydroxyuracil, exhibit sequence context-dependent mispairing *in vitro*. Nucleic Acids Research 1994; 22 (1): 72–78.
65. Fujii J, Iuchi Y, Okada F. Fundamental roles of reactive oxygen species and protective mechanisms in the female reproductive system. Reprod Biol Endocrinol 2005; 3: 43.
66. Conti CJ. Mechanisms of tumor progression, in: I.G. Sipes, C.A. McQueen, A.J. Gandolfi (Eds.), Comprehensive Toxicology 1997; 12: 383 – 400.
67. Peltola V, Mantyla E, Huhtaniemi I, Ahotupa M. Lipid peroxidation and antioxidant enzyme activities in the rat testis after cigarette smoke inhalation or administration of polychlorinated biphenyls or polychlorinated naphthalenes. J Androl 1994; 5(4):353-61.
68. Bhatia AL, Manda K. Study of pre-treatment of melatonin against radiation-induced oxidative stress in mice. Environ Toxicol Pharmacol 2004; 18(1):13-20.
69. Mills GC. Glutathione peroxidase and the destruction of hydrogen peroxide in animal tissues. Archives of Biochemistry and Biophysics 1960; 86 (1): 1 - 5.
70. Schmidtler W. Lysosomal enzymes in the oogenesis and folliculogenesis of the guinea pig (author's transl). Histochemistry 1980; 70(1): 77-90.
71. Tamate K, Sengoku K, Ishikawa M. The role of superoxide dismutase in the human ovary and fallopian tube. J Obstet Gynaecol 1995; 21(4): 401-9.
72. Zhang F, Wang C, Huang J, Zhong J, Shi F. Progress in the study on prolactin receptor. Acta Ecol Anim Domastici 2009; 30:6–9.
73. Xu R, Jiang D. Effect of hormone on hormone receptor. Prog Physiol Sci 1983; 14: 153–8.